APPLIED PHYSICS LETTERS **101**, 253519 (2012)

Polarization effects on gate leakage in InAlN/AlN/GaN high-electron-mobility transistors

Satyaki Ganguly,[a)] Aniruddha Konar, Zongyang Hu, Huili Xing, and Debdeep Jena
Department of Electrical Engineering, University of Notre Dame, Notre Dame, Indiana 46556, USA

(Received 27 September 2012; accepted 10 December 2012; published online 21 December 2012)

Lattice-matched InAlN/AlN/GaN high electron mobility transistors offer high performance with attractive electronic and thermal properties. For high-voltage applications, gate leakage currents under reverse bias voltages remain a serious challenge. This current flow is dominated by field enhanced thermal emission from trap states or direct tunneling. We experimentally measure reverse-bias gate leakage currents in InAlN/AlN/GaN transistors at various temperatures and find that the conventional trap-assisted Frenkel-Poole model fails to explain the experimental data. Unlike the non-polar semiconductors Si, Ge, large polarization-induced electric fields exist in III-nitride heterojunctions. When the large polarization fields are accounted for, a modified Frenkel-Poole model is found to accurately explain the measured data at low reverse bias voltages. At high reverse bias voltages, we identify that the direct Fowler-Nordheim tunneling mechanism dominates. The accurate identification of the gate leakage current flow mechanism in these structures leads to the extraction of several useful physical parameters, highlights the importance of polarization fields, and leads to suggestions for improved behavior. © *2012 American Institute of Physics*. [http://dx.doi.org/10.1063/1.4773244]

High spontaneous and piezoelectric polarization charges at heterojunctions coupled with a large bandgap propel GaN high electron mobility transistors (HEMTs) to outperform Si devices for high-speed power switching. The lattice matched $In_{0.17}$ $Al_{0.83}$N barrier GaN HEMTs[1] is a suitable candidate for that due to its promising electronic properties and thermal stability. An AlN interlayer[2] is necessary in InAlN HEMTs to boost the mobility of the two-dimensional electron gas (2DEG) channel by reducing alloy scattering. Although high performance InAlN/AlN/GaN HEMTs have been reported, reverse-bias gate leakage remains a pressing issue. This is a serious problem affecting the use of InAlN heterostructures for high-voltage switching.[3] The identification of the physical origin of gate leakage in these structures is essential at this stage for progress, and is the subject of this work. We show that incorporation of the large polarization field is essential to understand gate leakage, a feature that has not been considered in prior works.

At high reverse-bias voltage on the gate, near and beyond threshold, electrons from the metal can tunnel into the 2DEG HEMT channel through a voltage-dependent triangular potential barrier as shown in Fig. 1(a). This is Fowler-Nordheim (FN) tunneling,[4] which we address later in this work. At low reverse-bias voltages on the gate, electrons from the metal must tunnel through the entire barrier to enter the HEMT 2DEG channel. This process would lead to a very low current in pure defect-free barrier layers. But due to the presence of trap states in the gap, field enhanced thermal emission results high leakage current as shown in Fig. 1(c). The process is identified as the trap-assisted Frenkel-Poole emission (FPE) mechanism.[5] We focus on this leakage mechanism first.

The experimental signature of FPE is obtained by measuring the temperature-dependence of the leakage current density $J(T)$ through the gate barrier at various values of the electric field F in the barrier. Based on Frenkel's original model[5] of electric-field assisted emission from trap states into a continuum of electronic states, the expression for the current density is

$$J(T) = CF\exp[-\phi_t/kT + A(T)\sqrt{F}], \quad (1)$$

where C is a constant, $F = V/d$ is the field in the barrier of thickness d when a voltage V drops across it, ϕ_t is the trap ionization energy, k is the Boltzmann's constant, and $A(T) = q(\sqrt{q/\pi\varepsilon_0\varepsilon_s})/kT$ is a coefficient with q as the electron charge, ε_0 the permittivity of free-space, and ε_s the relative high-frequency dielectric permittivity of InAlN barrier. One should note that it has been assumed here that the filling of the trap states from gate metal via tunneling does not limit the electric field enhanced emission process.

Thus, according to the original FPE model, the dependence of $\log[J(T)/F]$ vs $\sqrt{F}$ should be linear. In prior reports[6,7] for InAlN/GaN heterostructures, this linear dependence is reported. However, the original FPE model also requires the slope of the linear behavior $A(T)$ vs $1/T$ to follow a straight line passing through the origin. This dependence is not precisely followed in the prior reports. Moreover, the extraction of ε_s and ϕ_t in the prior reports is questionable owing to the ambiguity of the near-surface electric field F used there. By comparing our own experimental data with the model, we trace the problem to the neglect of the polarization field. The proper accounting of the zero bias polarization induced electric field F_π within the InAlN barrier demands a modification of the original FPE expression. We propose such a modified FPE expression, and use it to accurately extract ϕ_t and ε_s in InAlN barrier layer from the

a)Author to whom correspondence should be addressed. Electronic mail: sganguly@nd.edu.

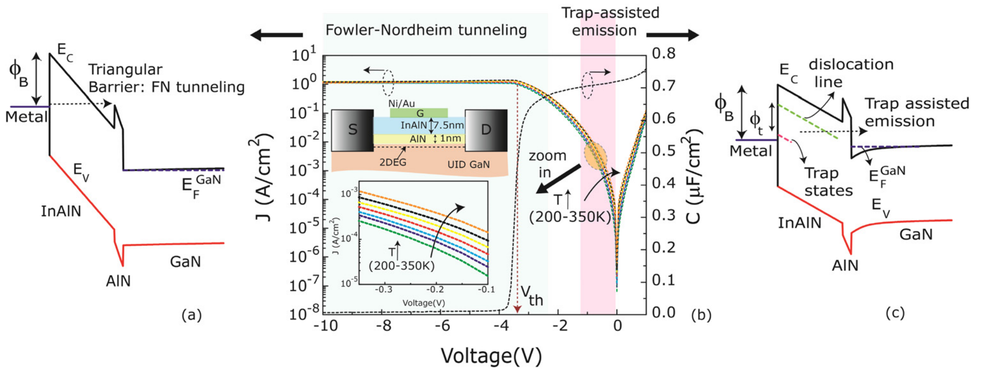

FIG. 1. J-V characteristics of the (Ni/Au)/InAlN/AlN/GaN diode measured at various temperatures. C-V plot (at 1 MHz) at RT is also shown. The band diagrams (1-D Poisson simulation) show Fowler-Nordheim tunneling at higher biases and trap assisted emission at lower biases dominate. The schematic of the diode structure and the zoomed-in view of the J-V characteristics to capture the temperature dependence prominently are shown in the inset.

measured data, in a consistent and more comprehensive picture. In addition, we find that at higher reverse biases FN tunneling dominates over the trap assisted emission. From the FN plots of the experimental data, we extract the Ni/InAlN surface barrier height ϕ_B and electron tunneling effective mass m^* in the barrier layer. The correct estimation of these parameters is expected to accelerate the choice of optimal gate stacks for InAlN HEMTs. Also based on the findings, we propose methods to reduce the severity of the gate leakage in InAlN structures for superior high-speed power switching.

The InAlN(7.5 nm)/AlN(1 nm)/GaN(2 μm) HEMT structures used were grown by metal-organic chemical vapor deposition (MOCVD) on SiC substrate at IQE RF LLC. Mesa isolation was performed followed by source/drain ohmic metallization using Ti/Al/Ni/Au (20/100/40/50 nm) stack deposition followed by rapid thermal annealing in N_2/Ar atmosphere for 18 s at 850 °C. A saturation current of $\sim$1.5 A/mm and a contact resistance of 0.4 Ω·mm were measured across ungated pads. Finally, Ni/Au (40/100 nm) gate metal stacks were deposited. A 2DEG sheet charge of 1.55×10^{13} cm^{-2} and an electron mobility of 1350 cm^2/Vs with a resultant sheet resistance of 290 ohm/sq were obtained by Hall-effect measurements at room temperature. The schematic layer structure of the processed sample is shown in the inset of Figure 1(b). Figure 1(b) also shows the T-dependent $J(T)$ vs V measurement on a Schottky diode with radius 20 μm over a temperature range of 200 K–350 K. The temperature dependence of current at low reverse bias voltages is explained by our modified FPE expression incorporating polarization-induced electric field in the barrier. The weak temperature-dependence and saturation of the gate current at high reverse biases are the consequence of FN tunneling, with the saturation of the vertical electric field beyond threshold.[8,9]

The capacitance-voltage curve shown in Figure 1(b) indicates that the 2DEG is depleted beyond the threshold voltage $V_{th} = -3.3$ V. The vertical electric field in the InAlN barrier is obtained using Gauss's law from the charge-diagram as shown in the inset of Fig. 2(a) as $F = q(P_{\pi(InAlN)} - P_{\pi(GaN)} - n_s)/\varepsilon_0\varepsilon_b$. Here, $P_{\pi(InAlN)} \sim 4.54 \times 10^{13}$ cm^{-2} (Ref. 1) is the InAlN polarization charge, $P_{\pi(GaN)} \sim 1.81 \times 10^{13}$ cm^{-2} (Ref. 1) is the GaN polarization charge, ε_b is the low-frequency dielectric constant, and n_s is the 2DEG density obtained from a self-consistent 1-D Poisson Schrödinger simulation[10] as a function of the applied gate voltage V. Owing to the depletion of the 2DEG near threshold, $n_s \rightarrow 0$, and the saturation electric field is then $F_{sat} = 4.7$ MV/cm. The calculated vertical field $F \rightarrow F_{sat}$ also levels off beyond V_{th} as shown in Fig. 2(a). Before saturation, in the linear region of the graph F can be expressed as $F = F_\pi + (V/d)$, where F_π is the zero-bias polarization-induced electric field in the

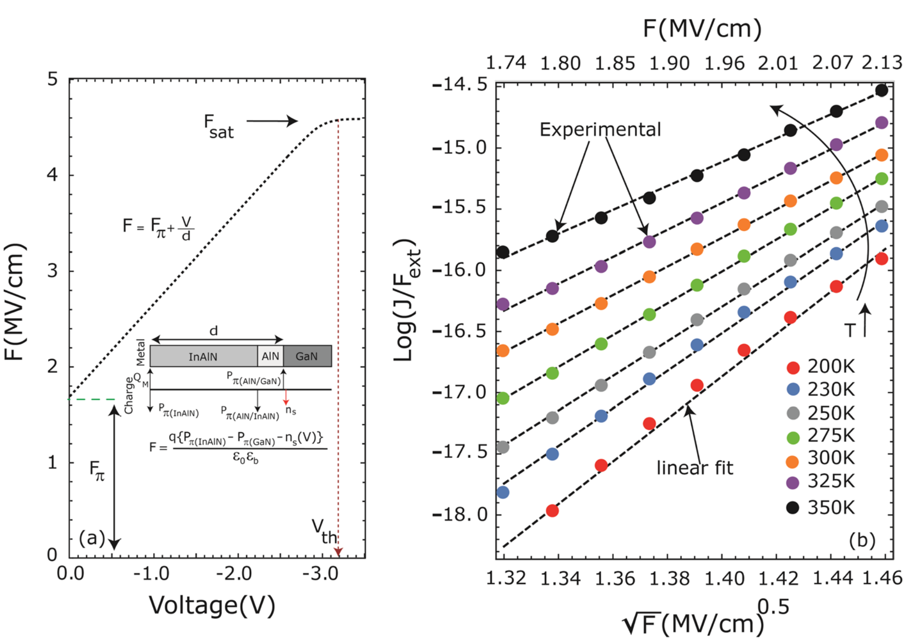

FIG. 2. (a) Calculated electric field at the InAlN barrier for different reverse bias voltages; the charge diagram and electric field as a function of 2DEG density is shown in the inset; (b) the evaluated $\log(J/F_{ext})$ vs $\sqrt{F}$ plot for various temperatures has been shown.

barrier. We first investigate the following modification to the original FPE expression in Eq. (1) for trap-assisted thermal emission to account for this polarization-induced field

$$J = C(F_\pi + V/d)\exp[(-\phi_t/kT + A(T)\sqrt{F_\pi + V/d})]. \quad (2)$$

However, in this expression, the net diode current density does not go to zero at $V = 0$. In Frenkel's original work,[5] the zero bias electric field was neglected—this is indeed justified in the non-polar semiconductors like Si, Ge, etc. In the analysis of gate leakage mechanisms in FETs made from these materials, the energy band bending at zero bias is assumed to be small compared to the applied voltage.[11] However, this is not the case for III-nitrides due to the built-in polarization field.

We, therefore, seek to correctly account for the presence of the large zero-bias field. Note that from Eq. (2) at $V = 0$, $J_0 = CF_\pi \exp(-\phi_t/kT)\exp[A(T)\sqrt{F_\pi}]$. If we assume that at $V = 0$, this current is balanced by a reverse current which obeys the same temperature and field dependence, then the modified expression for FPE (MFPE) at any reverse bias voltage is given by

$$J = C\exp(-\phi_t/kT) \cdot (F\exp[A(T)\sqrt{F}] - F_\pi \exp[A(T)\sqrt{F_\pi}]), \quad (3)$$

where $F = F_\pi + V/d$. This expression indeed meets the zero-bias criterion. For low bias voltages, i.e., when $V/d \ll F_\pi$, the MFPE expression approximates by a Taylor expansion to,

$$J \approx C^*(V/d)\exp(-\phi_t/kT)[\exp(A(T)\sqrt{F})], \quad (4)$$

where $C^* = [1 + (A(T)\sqrt{F_\pi})/2]C$ is a modified coefficient. From Eq. (4), if the current transport is dominated by trap states at low reverse bias voltages, $\log(J/F_{ext})$ with $F_{ext} = V/d$ should be a linear function of $\sqrt{F}$, as confirmed in Figure 2(b).

Since $\log(J(T)/F_{ext}) = A(T)\sqrt{F} - \phi_t/kT + \log C^*$, the coefficient $A(T)$ is extracted from the slope, and $-\phi_t/kT + \log C^* (= B(T))$ from the intercept of the $\log(J(T)/F_{ext}) - \sqrt{F}$ plot. The reverse-bias voltage range used is 0 to -0.5 V, which sweeps the vertical field over the range shown in Fig. 2(b), and the data highlights the scans over 200 K–350 K temperature range. The linear behavior *and* the temperature-dependent slopes signifying the coefficient $A(T)$ are evident. Since $A(T) = q(\sqrt{q/\pi\varepsilon_0\varepsilon_s})/kT$, a plot of $A(T)$ against $1/T$ should yield a straight line of the type "$y = mx$" passing through the origin. The slope of this line should give us the value of ε_s. Figure 3(a) shows that is, indeed, the case. The obtained value of $\varepsilon_s \sim 6.2$ in this case is in good agreement with the extrapolated value for InAlN, since $\varepsilon_{AlN} = 4.77$, $\varepsilon_{InN} = 8.4$.[12] This is the first report where the proposed MFPE given in Eqs. (3) and (4) accurately captures the variation of $A(T)$ against $1/T$ and yields a reasonable value of ε_s. The reason can be traced to the proper accounting of the large polarization-induced electric field in the barrier.

Similarly, we take the intercepts and from the slope of the $-\phi_t/kT + \log C^*$ vs $1/T$ plot, we find $\phi_t \sim 0.48$ eV as shown in Fig. 3(b). The higher value of ϕ_t obtained here as compared to previous reports[6,7] could be due to the more accurate and rigorous model used in this work where electric field in the barrier has been properly taken into account. Now if the MFPE dominated current finds a path through the conductive dislocations[13] present in InAlN (Fig. 1(c)), then those dislocations would lie $\phi_t = 0.48$ eV above the trap state levels, assuming these traps lie very close to the metal Fermi level. Since if the trap levels are significantly lower in energy then direct emission of carriers from the gate into conductive dislocations can dominate. On the other hand, if the trap level energies are significantly higher, then the filling of the traps can become a significant factor. The conductive AFM image of InAlN surface shown in the inset of Figure 3(b) confirms the presence of conductive dislocations ($\sim 5 \times 10^8$ cm^{-2}) in these heterostructures. A similar explanation was given by Zhang *et al.*[14] in case of AlGaN/GaN heterostructures. Since dislocations form localized paths, they can be considered crudely as "area defects" only for large-area gates that contain lots of them. Though at this stage we have not conclusively identified the exact *nature* of defects that are responsible for MFPE at low voltages, we have shown that it is essential to include polarization to explain the experimentally measured currents with this mechanism.

At higher reverse-bias gate voltages as indicated in Fig. 1(a), the effective barrier for electron tunneling becomes

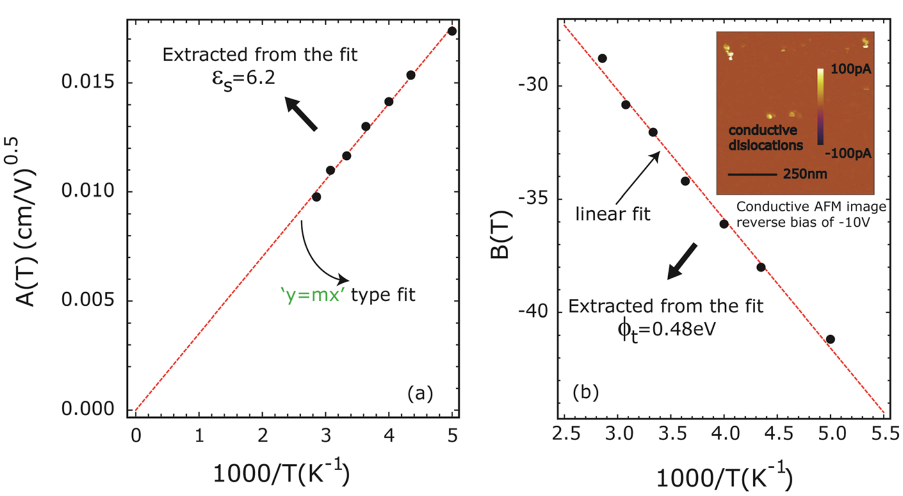

FIG. 3. (a) Extracted $A(T)$ vs $(1000/T)$ for various temperatures has been plotted. The data points have been fitted with a straight line of "$y = mx$;" (b) Extracted $B(T)$ vs $(1000/T)$ for various temperatures have been plotted. Conductive AFM image of the InAlN surface has been shown in the inset.

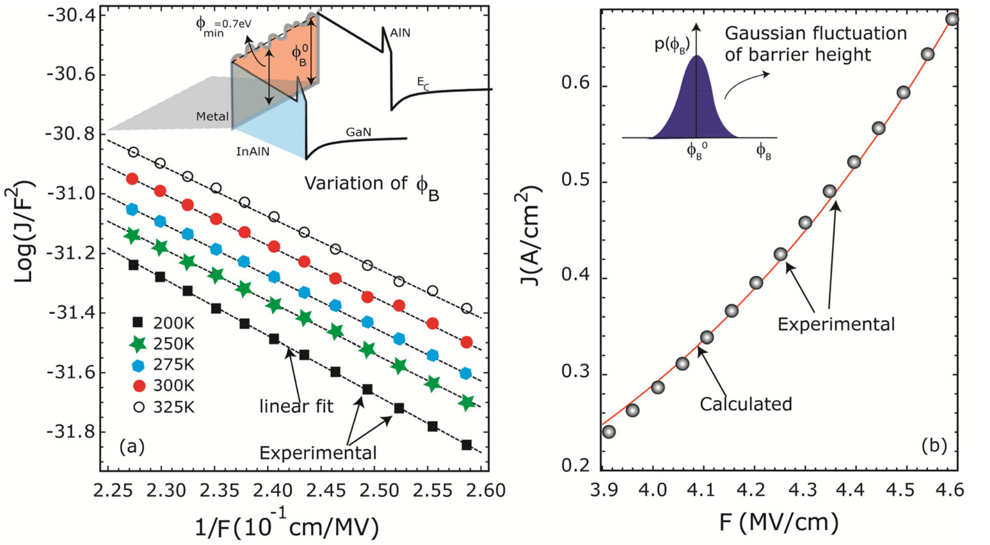

FIG. 4. (a) The evaluated $\log(J/F^2)$ vs $1/F$ plot for various temperatures has been shown. Fluctuations of surface barrier height due to In segregation have been shown in the inset; (b) experimental and calculated current densities (FN dominated), which take into account the variation of ϕ_B are plotted.

triangular and direct FN tunneling starts to dominate over MFPE. The FN tunneling current density is given by

$$J(\phi_B) = K_1 F^2 \exp[-K_2(\phi_B)/F], \tag{5}$$

where K_1 is the proportionality constant and $K_2 = 8\pi\sqrt{2m_T^*\phi_B^3}/3qh$. Here ϕ_B is the effective barrier height at the Schottky metal contact, h is the Planck's constant, and m_T^* is the electron tunneling effective mass in the InAlN barrier. The linearity of the $\log(J/F^2)$ vs $1/F$ plots for various temperatures, combined with their temperature-independent slopes shown in Fig. 4(a) are signatures of FN tunneling. We extract the tunneling effective mass to be $m_T^* \sim 0.2m_e$, and the effective barrier height of the Schottky contact is found to be $\phi_B \sim 0.7$ eV. The barrier height is lower than the previous report.[15] This low value of the surface barrier height can be attributed to microscopic In composition fluctuations in InAlN and which could depend well on the growth and subsequent surface treatment.

Since the bandgaps of InN and AlN are vastly different, compositional fluctuations[13] in the InAlN barrier layer will lead to an effective band-diagram at the metal/InAlN interface as shown in the inset of Fig. 4(a). As the FN current has a strong exponential dependence on ϕ_B, the current will tunnel through regions of the *lowest surface barrier height*. As a result, our extracted value of ϕ_B represents a lower limit of the surface barrier height of InAlN. To accurately capture the barrier fluctuation, a Gaussian probability distribution[16] of barrier height $p(\phi_B) = (1/\sqrt{2\pi\sigma})\exp[-(\phi_B - \phi_B^0)/2\sigma^2]$ is assumed, where ϕ_B^0 is the average barrier height and σ is the standard deviation, the FN current density is calculated averaging over all possible values of ϕ_B as $\langle J_{FN}\rangle = \int J(\phi_B)p(\phi_B)d\phi_B$, where $J(\phi_B)$ is defined in Eq. (5). The current density calculated from the above expression in the voltage range -2.2 V to -2.9 V matches well with the experimental data shown in Fig. 4(b) for the choices $\phi_B^0 = 1.56$ eV and $\sigma = 0.29$ eV. The average surface barrier height ϕ_B^0 obtained here matches well with the previously reported[15] surface barrier height of Ni/InAlN. The slight temperature dependence observed in the FN plots in Fig. 4(a) can be explained by considering the Fermi-Dirac distribution[17] for the electrons in the conduction band of the gate metal. This consideration introduces a multiplicative term into the expression of current given by $J(\phi_B) = [(\pi akT)/\sin(\pi akT)]\, K_1F^2\exp[-K_2(\phi_B)/F]$, where $a = 4\pi\sqrt{(2m_T^*\phi_B)}t(y)/hqF$, and $t(y)$ is a tabulated elliptic integral where $y = (1/\phi_B)\sqrt{(q^3F/4\pi\varepsilon_0\varepsilon_b)}$. This correction term causes the slight parallel shift in the FN plots as seen in Figure 4(a). To combine the findings at various bias conditions, Fig. 5 shows the plot of the measured room temperature gate current density, together with the calculated gate current using the proposed MFPE in Eq. (3), and FN tunneling of Eq. (5) using the extracted parameters. The separate agreements in the low-bias and the high bias conditions suggest the accuracy of our approach.

To conclude, we have shown the importance of properly accounting for the built-in polarization-induced electric fields in GaN HEMTs in understanding gate leakage

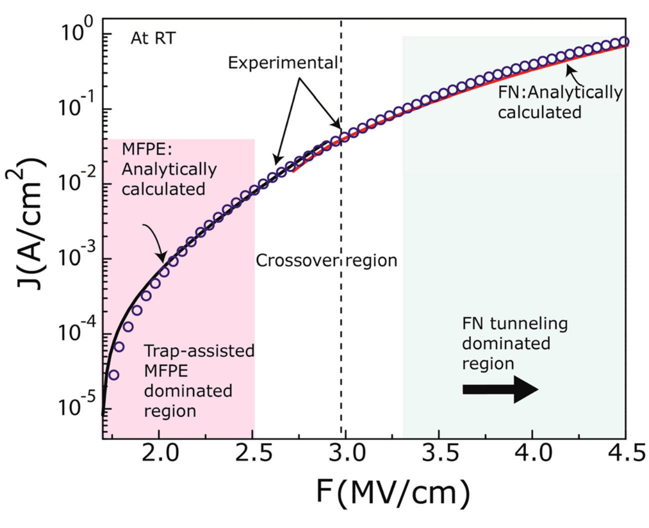

FIG. 5. Experimental and calculated current densities using proposed MFPE and FN tunneling expression. At low field, MFPE matches the experimental data, whereas at high field the tunneling transport is FN dominated.

currents. The trap-assisted emission and direct FN tunneling mechanisms are strong functions of the effective barrier height at the InAlN/Schottky metal contact interface. Hence to suppress the severity of the leakage current in these heterostructures it is necessary to alter the top barrier layer. For example, the Ni/AlN surface barrier height[18] of $\sim 3\,\mathrm{eV}$ is much larger than that of Ni/InAlN barriers obtained in this work. A thin AlN cap layer on the InAlN barrier can reduce the gate leakage current by a substantial amount. In addition, it can reduce the band-edge fluctuations in InAlN, since AlN is a binary semiconductor. The introduction of a high bandgap, crystalline, and thin AlN cap layer can thus reduce the gate leakage substantially and extend the voltage switching capability of InAlN HEMTs.

The authors acknowledge Financial support from the DARPA MPC program.

[1]J. Kuzmík, IEEE Electron Device Lett. **22**, 510 (2001).
[2]R. Butte, J.-F. Carlin, E. Feltin, M. Gonschorek, S. Nicolay, G. Christmann, D. Simeonov, A. Castiglia, J. Dorsaz, H. J. Buehlmann, S. Christopoulos, H. von Högersthal, A. J. D. Grundy, M. Mosca, C. Pinquier, M. A. Py, F. Demangeot, J. Frandon, P. G. Lagoudakis, J. J. Baumberg, and N. Grandjean, J. Phys. D: Appl. Phys. **40**, 6328 (2007).
[3]J. Kuzmík, A. Kostopoulos, G. Konstantinidis, J.-F. Carlin, A. Georgakilas, and D. Pogany, IEEE Trans. Electron Devices **53**, 422 (2006).
[4]J. G. Simmons, J. Phys. D: Appl. Phys. **4**, 613 (1971).
[5]J. Frenkel, Phys. Rev. **54**, 647 (1938).
[6]E. Arslan, S. Bütün, and E. Ozbay, Appl. Phys. Lett. **94**, 142106 (2009).
[7]S. Pandey, D. Cavalcoli, B. Fraboni, A. Cavallini, T. Brazzini, and F. Calle, Appl. Phys. Lett. **100**, 152116 (2012).
[8]E. J. Miller, X. Z. Dang, and E. T. Yu, J. Appl. Phys. **88**, 5951 (2000).
[9]D. Yan, H. Lu, D. Cao, D. Chen, R. Zhang, and Y. Zheng, Appl. Phys. Lett. **97**, 153503 (2010).
[10]I. H. Tan, G. L. Snider, L. D. Chang, and E. L. Hu, J. Appl. Phys. **68**, 4071 (1990).
[11]S. M. Sze, *Physics of Semiconductor Devices*, 3rd ed. (Wiley, New York, 1981), Chap. 4.
[12]C. Wood and D. Jena, *Polarization Effects in Semiconductors*, 1st ed. (Springer, New York, 2007), Chap. 4.
[13]J. Song, F. J. Xu, X. D. Tan, F. Lin, C. C. Huang, L. P. You, T. J. Yu, X. Q. Wang, B. Shen, K. Wei, and X. Y. Liu, Appl. Phys. Lett. **97**, 232106 (2010).
[14]H. Zhang, E. J. Miller, and E. T. Yu, J. Appl. Phys. **99**, 023703 (2006).
[15]D. Donoval, A. Chvála, R. Šramatý, J. Kováč, J.-F. Carlin, N. Grandjean, G. Pozzovivo, J. Kuzmík, D. Pogany, G. Strasser, and P. Kordoš, Appl. Phys. Lett. **96**, 223501 (2010).
[16]L. Zheng, R. P. Joshi, and C. Fazi, J. Appl. Phys. **85**, 3701 (1999).
[17]M. Lenzlinger and E. H. Snow, J. Appl. Phys. **40**, 278 (1969).
[18]D. Qiao, L. S. Yu, S. S. Lau, J. M. Redwing, J. Y. Lin, and H. X. Jiang, J. Appl. Phys. **87**, 801 (2000).